



Adsorption of ionic liquid onto halloysite nanotubes: Thermal and mechanical properties of heterophasic PE-PP copolymer nanocomposites

E. Bischoff, D. A. Simon, S. A. Liberman, and R. S. Mauler

Citation: [AIP Conference Proceedings](#) **1713**, 090004 (2016); doi: 10.1063/1.4942300

View online: <http://dx.doi.org/10.1063/1.4942300>

View Table of Contents: <http://scitation.aip.org/content/aip/proceeding/aipcp/1713?ver=pdfcov>

Published by the [AIP Publishing](#)

Articles you may be interested in

[Dielectric analysis of halloysite nanotubes LLDPE nanocomposite compounds](#)

AIP Conf. Proc. **1713**, 090007 (2016); 10.1063/1.4942303

[Optical and mechanical properties of UV-weathered biodegradable PHBV/PBAT nanocomposite films containing halloysite nanotubes](#)

AIP Conf. Proc. **1599**, 398 (2014); 10.1063/1.4876862

[Barrier properties of PE, PP and EVA \(nano\)composites - The influence of filler type and concentration](#)

AIP Conf. Proc. **1599**, 186 (2014); 10.1063/1.4876809

[Mechanical properties of PE, PP, Surlyn and EVA/clay nanocomposites for packaging films](#)

AIP Conf. Proc. **1599**, 178 (2014); 10.1063/1.4876807

[Gamma radiation induced degradation in PE-PP block copolymer](#)

AIP Conf. Proc. **1447**, 151 (2012); 10.1063/1.4709925

Adsorption of Ionic Liquid onto Halloysite Nanotubes: Thermal and Mechanical Properties of Heterophasic PE-PP Copolymer Nanocomposites

E. Bischoff^a, D.A. Simon^{a, b}, S.A. Liberman^a and R.S. Mauler^{a*}

^a*Institute of Chemistry, Universidade Federal do Rio Grande do Sul – UFRGS, Av. Bento Gonçalves, 9500, Porto Alegre 91501-970 RS, Brazil*

^b*Federal Institute of Rio Grande do Sul – IFRS-Campus Farroupilha, Av. São Vicente, 785, Farroupilha, 95180-000 RS, Brazil*

eve_bischoff@yahoo.com.br
raquel.mauler@ufrgs.br

Abstract. The surface adsorption of inorganic clays with ionic liquids has attracted much attention due to improve the interaction of hydrophilic clay with the hydrophobic polymers. However, successful organic adsorption strongly depends on the characteristics of ionic liquid (anion, chain size and concentration), and the reaction conditions (as polarity of solvent). In this study, such factors were analyzed and correlated with morphology, thermal and mechanical properties of the nanocomposites. The heterophasic ethylene-propylene copolymer nanocomposites were prepared by melt intercalation method in a twin screw co-rotating extruder. The halloysite nanotubes (HNT) was used as filler – natural and modified with different ionic liquids. The results showed that a better distribution and dispersion of the nanoparticles was achieved in the samples with modified HNT (m-HNT) and was more significant when the ionic liquid adsorption was conducted in a less polar solvent. The thermal stability of the nanocomposites with m-HNT was higher compared to the neat CP. Additionally, the better balance in the mechanical properties was obtained by the use of the more hydrophobic ionic liquid and higher concentration with improve of 27% in the Young Modulus without loss in the impact properties at room temperature. These superior behaviors of ionic liquid adsorption products exhibit properties suitable for many industrial applications.

Keywords: Ionic liquids, HNT, Dispersion, Copolymer

INTRODUCTION

Polypropylene (PP) is a widely applied thermoplastic polymer because of its versatile properties, including low density and cost, good processability and recyclability [1], though the low fracture toughness is a limitation. The use of heterophasic ethylene-propylene copolymers (CP) may change this panorama, as CP consists of a semi-crystalline isotactic PP homopolymer matrix with a soft ethylene-propylene rubber (EPR) dispersed phase [2]. This dispersed elastomer phase serves to improve the toughness and low-temperature impact resistance of PP. Inevitably, the elastomeric component has a detrimental effect on the stiffness of the material [3]. One way to achieve the desired property-balance could be the addition of small amounts of rigid nanoparticles [4].

Polymer nanocomposites have been extensively studied due to the premise of better mechanical, electrical and thermal properties compared to pure polymer or “traditional composites” [5, 6]. In general, the key factors for obtaining advanced performance polymer nanocomposites are homogeneous distribution of nanofiller within the polymer matrix, and a strong interfacial adhesion between matrix and nanofiller [7]. Nevertheless, the chemical affinity between inorganic fillers of hydrophilic nature and nonpolar hydrophobic polymers is low, which could be compatibilized by surface modification of the filler [8, 9].

Among the broad variety of inorganic fillers applied for the preparation of polymer nanocomposites, halloysite nanotubes (HNT) received much attention in the last years [10]. HNT, having the molecular formula of $\text{Al}_2\text{Si}_2\text{O}_5(\text{OH})_4 \cdot n\text{H}_2\text{O}$, are naturally occurring multi-walled inorganic nanotubes with high aspect

ratio [11], showing a similar geometry to that of carbon nanotubes [12]. The HNT dimensions depend on the deposits, showing lengths in the range of 1–15 μm ; inner diameters of 10–30 nm and outer diameter of 50–70 nm [13]. In contrast to most other clays, the majority of the aluminols are located in the interior of the HNT, while the outer surface of the HNT are primary siloxanes, and few silanols/aluminols are exposed at the edges of the sheets [14]. Due to the presence of these polar groups, HNT are extremely hydrophilic at its surfaces, the organomodification is of great interest for application as filler in the nanocomposites field [15].

Clay modification with ionic liquids (IL) has been explored as a way to improve clay dispersion in polymer matrices, thus increasing the final properties of resultant polymer nanocomposites. Within this context, this report addresses the role of ionic liquid as surface modifiers of HNT (m-HNT) in the preparation of compatibilized CP/HNT nanocomposites with improved performances.

EXPERIMENTAL

Materials

Braskem S.A. (Brazil) supplied CP with a melt flow index of 27.7 g/10 min (230 °C/2.16 kg) and total ethylene content of approximately 14 wt.-%. HNT was acquired from Sigma-Aldrich. The ionic liquids used (Table 1) were produced by Ionic Liquids Technologies GmbH.

TABLE 1: Name and composition of ionic liquids

Ionic Liquid	Abreviation	Composition	M.w (g.mol ⁻¹)
1-Decyl-3-methylimidazolium Tetrafluoroborate	C ₁₀ BF ₄	C ₁₄ H ₂₇ BF ₄ N ₂	310.18
1-Decyl-3-methylimidazolium bis(trifluoromethylsulfonyl)imide	C ₁₀ NTf ₂	C ₁₆ H ₂₇ F ₆ N ₃ O ₄ S ₂	503.53
1-Methyl-3-octadecylimidazolium bis(trifluoromethylsulfonyl)imide	C ₁₈ NTf ₂	C ₂₄ H ₄₃ F ₆ N ₃ O ₄ S ₂	615.74

Adsorption of IL onto HNTs

For the adsorption, approximately 20 g of HNT was dispersed in 120 mL of dry Acetone (A) or Dichloromethane (D) and 0.0032 mol of ionic liquid was added (0,0064 mol for the double concentration sample). The suspension was refluxed under inert atmosphere at 60 °C for 20 h with constant stirring. All m-HNT samples were collected in a Buchner funnel, filtered and washed with dry acetone or dichloromethane to remove non-reacted ionic liquid. Finally, all m-HNT were dried at room temperature for 24 h and under vacuum at 70 °C until a constant weight were reached.

Melt processing of CP nanocomposites

The CP nanocomposites with 2.0 wt.% of nanofiller were processed using a twin screw co-rotating extruder (Coperion ZSK18K38, screw diameter of 18 mm, L/D = 44), operating at 100 rpm with a constant feed ratio of 2.5 kg/h and a temperature profile of 150, 160, 165, 170, 175, 180, 185 °C. The nanocomposites were injection molded in a Battenfeld Plus 350/075 injection molding machine, keeping the temperature of the barrel between 210 and 230 °C, and the mold was maintained at 60 °C. For comparison, neat CP and CP nanocomposites with unmodified HNT were also processed under the same conditions. Samples are identified with IL used followed by A for Acetone or D for Dichloromethane (sample with double concentration have a number 2 before IL).

Characterization of CP/HNT nanocomposites

TEM (JEOL JEM-120 Ex II) was used to examine the morphology, operating at an accelerating voltage of 80 kV. Ultrathin specimens (~70 nm) were cut from the middle section of injection-molded specimens, in the perpendicular direction to the melt flow, under cryogenic conditions with a RMC CRX microtome. The

microtome was equipped with a glass or diamond knife at $-80\text{ }^{\circ}\text{C}$, and the film was retrieved onto 300 mesh Cu grids.

Films for DSC and TGA analysis were obtained by compression molding at $190\text{ }^{\circ}\text{C}$. Thermal properties were determined under a nitrogen atmosphere, using a DSC Thermal Analyst 2100/TA Instruments. The samples were heated from 40 to $200\text{ }^{\circ}\text{C}$ at a heating and cooling rate of $10\text{ }^{\circ}\text{C}/\text{min}$. Thermogravimetric analyses were carried out using a TA model QA-50 instrument to obtain the decomposition profiles of CP nanocomposites. The samples were heated under a nitrogen flow from 30 to $700\text{ }^{\circ}\text{C}$ at a rate of $20\text{ }^{\circ}\text{C}/\text{min}$.

The mechanical properties of the nanocomposites were evaluated through tensile and impact strength testing. Tensile tests were performed according to ASTM D638, specimen type I, on an universal tensile machine (EMIC DL 10000 with extensometer) at a speed of $50\text{ mm}/\text{min}$. Izod Impact tests were performed at $23\text{ }^{\circ}\text{C}$ using a pendulum-type impact tester (Ceast, Resilimpact), according to ASTM D256. In both cases, six specimens were analyzed, calculating the average and standard deviation.

RESULTS

Morphology

TEM micrograph of the CP/HNT (Fig. 1a) shows the presence of some agglomerates with a poor distribution of the clay particles exhibiting compact nanotubes, consisting of various aluminosilicate sheets, curved and closely packed with each other [16]. This confirms that only the shear forces during the processing are insufficient to promote dispersion of the untreated clay particles. The morphologies obtained for CP/m-HNT nanocomposites (Fig. 1b-f), despite the presence of some occasional agglomerates, show significant improvements in the dispersion and more homogeneous filler distributions, independent of the solvent, highlighting the role of the treatment with IL of hydrophilic HNT surfaces.

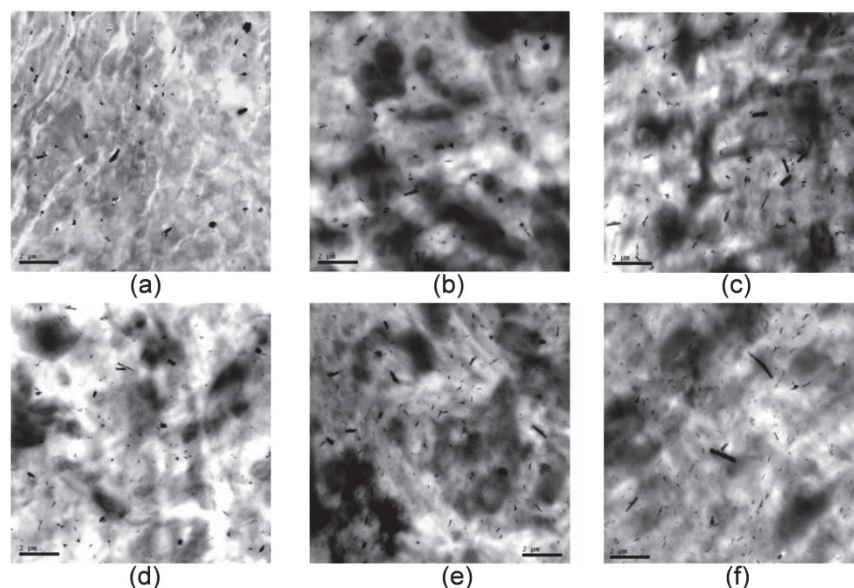


FIGURE 1. TEM images of (a) CP/HNT (b) CP/m-HNT $\text{C}_{10}\text{BF}_4\text{-A}$ (c) CP/m-HNT $\text{C}_{10}\text{BF}_4\text{-D}$ (d) CP/m-HNT $\text{C}_{10}\text{NTf}_2\text{-D}$ (e) CP/m-HNT $\text{C}_{18}\text{NTf}_2\text{-D}$ (f) CP/m-HNT $2\text{C}_{18}\text{NTf}_2\text{-D}$.

When comparing the solvents used for the preparation of m-HNT, slight morphological differences were observed in the final nanocomposites (Fig. 1b and c). For CP/m-HNT, the use of dichloromethane seems to have induced a higher level of adsorption of the IL C_{10}BF_4 on the HNT surface. Mroziak et al. [17] argued that IL may dominantly be absorbed on HNT surface through hydrogen bonding between surface siloxane and

hydrogens on the imidazolium ring. Due to the lower dielectric constant, the interaction of dichloromethane with IL is smaller when compared to acetone, which enables the ionic liquid is more available to interact with HNT surface. Consequently, a stronger interaction between the HNT and IL and the CP polymer chains was reached, showing a better distribution of the clay particles.

The type of the anion and length of the alkylsilane compatibilizer exerts a neglectable influence on the morphology of the nanocomposites (CP/m-HNT C₁₀NTf₂-D and CP/m-HNT C₁₈NTf₂-D), since the dispersion of the filler within the matrix showed no significant differences (Fig. 5d-e). The application of m-HNT 2C₁₈NTf₂-D with a double IL concentration (Fig. 1f) promoted a better distribution with the presence of small bundles and single dispersed nanotubes.

Mechanical Properties

The Young's Modulus and impact strength at 23 °C of neat CP and its nanocomposites are shown in Fig. 2, and all nanocomposites are afforded with increased Young's Modulus. The improvements in the Young's Modulus is generally attributed to the high stiffness and high aspect ratio of the HNT [18], which is also related to the degree of dispersion and the interaction of the clay with the matrix [7].

For nanocomposites obtained with m-HNT the impact strength presented different results depending on the IL used. The nanocomposites prepared with C₁₀BF₄ (CP/m-HNT C₁₀BF₄-A and CP/m-HNT C₁₀BF₄-D) obtained a significant decrease in impact strength, independent of the solvent used. On the other hand, for the CP/m-HNT C₁₀NTf₂-D a slight increase was reached when compared neat CP. The use of an IL with higher chain size (CP/m-HNT C₁₈NTf₂-D) promoted an increase in elastic modulus, consequently the higher rigidity of the material causes a reduction on impact properties. The use of double concentration of IL in the CP/m-HNT 2C₁₈NTf₂-D promoted improves in the elastic modulus without loss in the impact strength and may be attributed to better interfacial adhesion between m-HNT and the CP matrix, allowing the IL to act effectively as compatibilizer.

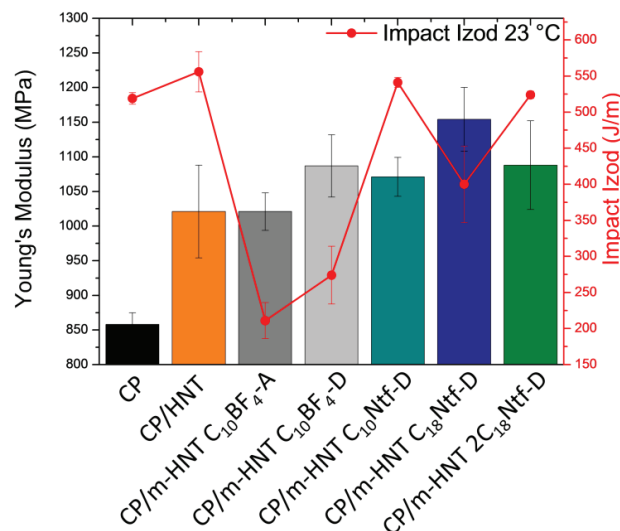


FIGURE 2. Mechanical properties of CP and CP nanocomposites.

Thermal Properties

The thermal stability of nanocomposites was evaluated by TGA analysis. Table 2 presents the characteristic temperatures T_{10%}, T_{50%} and T_p, which correspond to the initial and final decomposition temperature (10 wt.-% and 50 wt.-% degradation) and the maximum degradation rate, respectively, for the CP nanocomposites with unmodified and modified HNT.

The CP/HNT nanocomposite presented a similar thermal behavior as the neat polymer, indicating no changes in the degradation mechanism. This can be attributed to the HNT agglomerates (shown in Fig. 1a),

which did not affect the thermal stability of CP [19]. For the nanocomposites obtained with m-HNT, the $T_{10\%}$, $T_{50\%}$ and T_p improved, and could be attributed the higher HNT dispersion that increases the length of the tortuous path that hinders the diffusion of decomposition gases [5].

TABLE 2. Thermal properties of CP and CP nanocomposites.

Sample	TGA (°C)			DSC (°C)	
	$T_{10\%}$	$T_{50\%}$	TP	T_m	T_c
CP	343	393	400	165	116
CP/HNT	338	395	408	165	117
CP/m-HNT C ₁₀ BF ₄ -A	362	420	433	166	118
CP/m-HNT C ₁₀ BF ₄ -D	369	432	452	166	118
CP/m-HNT C ₁₀ NTf ₂ -D	344	400	412	165	118
CP/m-HNT C ₁₈ NTf ₂ -D	358	420	427	165	118
CP/m-HNT 2C ₁₈ NTf ₂ -D	364	420	433	166	118

The HNT and m-HNT nanoparticles did not affect the melt behavior (T_m) of the nanocomposites. In contrast, the halloysite incorporation affected slightly the crystallization temperature, increasing from 116 °C for neat CP to 118 °C for m-HNT nanocomposites. The halloysite filler acts as nucleation agent and better the clay dispersion within the matrix, larger the number of nuclei, affecting the crystallization temperature.

CONCLUSIONS

The adsorption of ionic liquid m-HNT in the preparation of CP nanocomposites led to a more homogeneous dispersion of the clay particles, increasing stiffness and thermal stability of samples. In addition, the application of m-HNT modified with a more hydrophobic ionic liquid in higher concentration promoted a better balance in mechanical properties and are suitable for many industrial applications.

ACKNOWLEDGEMENTS

The authors are grateful to CAPES, CNPq, Finep and FAPERGS/PRONEX for their financial support.

REFERENCES

1. D. Kaempfer, R. Thomann, R. Mülhaupt, *Polymer*, **43**, 2909-2916, (2002).
2. M. Koosha, N. Ebrahimi, Y. Jahani, S. A. S. Sajjadi, *Radiat Phys Chem*, **80**, 810-816, (2011).
3. J. Wang, Q. Dou, *Polym Int*, **57**, 233-239, (2008).
4. R. R. Tiwari, D. Paul, *Polymer*, **52**, 5595-5605, (2011).
5. K. Santos, E. Bischoff, S. Liberman, M. Oviedo, R. Mauler, *Ultrason Sonochem*, **18**, 997-1001, (2011).
6. Y. Li, J. Tang, L. Huang, Y. Wang, J. Liu, X. Ge, S. C. Tjong, R. K. Y. Li, L. A. Belfiore, *Composites Part A*, (2014).
7. H. Ismail, S. Salleh, Z. Ahmad, *Mater Des*, **50**, 790-797, (2013).
8. K. Santos, S. Liberman, M. Oviedo, R. Mauler, *J Polym Sci, Part B: Polym Phys*, **46**, 2519-2531, (2008).
9. Y.-J. Wan, L.-X. Gong, L.-C. Tang, L.-B. Wu, J.-X. Jiang, *Composites Part A*, **64**, 79-89, (2014).
10. J. Marini, E. Pollet, L. Averous, R. E. S. Bretas, *Polymer*, (2014).
11. L. N. Carli, J. S. Crespo, R. S. Mauler, *Composites Part A: Applied Science and Manufacturing*, **42**, 1601-1608, (2011).
12. P. Pasbakhsh, G. J. Churchman, J. L. Keeling, *Appl Clay Sci*, **74**, 47-57, (2013).
13. S. Ranganatha, T. V. Venkatesha, K. Vathsala, *Appl Surf Sci*, **263**, 149-156, (2012).
14. M. Liu, Z. Jia, D. Jia, C. Zhou, *Prog Polym Sci*, (2014).
15. P. Yuan, P. D. Southon, Z. Liu, M. E. R. Green, J. M. Hook, S. J. Antill, C. J. Kepert, *The Journal of Physical Chemistry C*, **112**, 15742-15751, (2008).
16. Y. Tang, L. Ye, S. Deng, C. Yang, W. Yuan, *Mater Des*, **42**, 471-477, (2012).
17. W. Mroziak, C. Jungnickel, M. Skup, P. Urbaszek, P. Stepnowski, *Environmental Chemistry*, **5**, 299-306, (2008).
18. B. Wang, H.-X. Huang, *Composites Part A*, **66**, 16-24, (2014).
19. B. Lecouvet, M. Sclavons, S. Bourbigot, J. Devaux, C. Bailly, *Polymer*, **52**, 4284-4295, (2011).